

RESEARCH PAPER

Characterization, cell toxicity, and antimicrobial activity of a carvacrol-encapsulating nanoliposomal system against *Staphylococcus aureus*, *Pseudomonas aeruginosa*, and *Escherichia coli*

Ali Majidi Yazdi¹, Arshad Hosseini^{1*}, Seyed Mohammad Gheibihayat², Mohammad Beygi³, Bibi Fatemeh Haghirsadat^{4*}, Fatemeh Oroojalian^{5,6*}

¹Department of Medical Biotechnology, School of Allied Medical Sciences, Iran University of Medical Sciences, Tehran, Iran

²Department of Medical Biotechnology, School of Medicine, Shahid Sadoughi University of Medical Sciences, Yazd, Iran

³Department of Agricultural Biotechnology, College of Agriculture, Isfahan University of Technology (IUT), Isfahan, Iran

⁴Biotechnology Research Center, International Campus, Yazd Reproductive Sciences Institute, Shahid Sadoughi University of Medical Sciences, Yazd, Iran

⁵Natural Products and Medicinal Plants Research Center, North Khorasan University of Medical Sciences, Bojnurd, Iran

⁶Department of Advanced Technologies, School of Medicine, North Khorasan University of Medical Sciences, Bojnurd, Iran

ABSTRACT

Objective(s): *Staphylococcus aureus*, *Pseudomonas aeruginosa*, and *Escherichia coli* are the main pathogenic bacteria involved in severe, polymicrobial, and multidrug-resistant infections. For these infections to be overcome, lipid-based nanoparticles and nanoformulations such as liposomes have demonstrated marked potential in fighting bacterial infections by delivering antibacterial drugs, fusing with bacterial membranes, and promoting the direct delivery of antibacterial agents to bacteria. This study assesses the antibacterial effects of various formulations of carvacrol (CV)-encapsulating nanoliposomes on *S. aureus*, *P. aeruginosa*, and *E. coli*. The study further evaluates the cytotoxicity of the fabricated nanoliposomal system against human foreskin fibroblast (HFF) cells.

Materials and Methods: Various formulations of the liposomal nanosystem were first prepared through the thin film hydration method utilizing different concentrations of soy phosphatidylcholine (SPC), cholesterol (Chol), and Tween 60. The formulations were then evaluated for drug entrapment efficiency and release profiles, and the optimum formulation was determined for the experiments. The optimum formulation was then structurally analyzed, and the cytotoxicity of free CV and encapsulated CV on both bacteria and HFF cells was evaluated.

Results: Microbial tests revealed that CV-LPs outperform free CV regarding their antibacterial effects on the studied bacterial strains, with the maximum inhibitory effect exerted on *S. aureus*, followed by *E. coli* and *P. aeruginosa*.

Conclusion: Furthermore, the MTT assay indicated that the cytotoxicity of CV against normal HFF cells was remarkably declined when it was encapsulated in the liposomal nanosystem.

Keywords: Antimicrobial effect, Carvacrol, Infection, Liposomes, Phytochemicals

How to cite this article

Majidi Yazdi A, Hosseini A, Gheibihayat SM, Beygi M, Haghirsadat BF, Oroojalian F. Characterization, cell toxicity, and antimicrobial activity of a carvacrol-encapsulating nanoliposomal system against *Staphylococcus aureus*, *Pseudomonas aeruginosa*, and *Escherichia coli*. *Nanomed J.* 2024; 11(1): 93-106. DOI: 10.22038/NMJ.2023.76136.1854

*Corresponding authors: Emails: hosseini.a@iums.ac.ir; fhaghirsadat@gmail.com; f.oroojalian@ut.ac.ir; Oroojalian.f@gmail.com

Note. This manuscript was submitted on September 9, 2023; approved on November 27, 2023

INTRODUCTION

Nanoparticles (NPs) and nanocarriers such as liposomal systems have demonstrated a significant impact against various diseases like

cancers, skin diseases, wounds, and microbial wound infections [1-4]. These nanomaterials offer unique advantages such as controlled and sustained drug release, increased drug half-life, and bioavailability, and can provide the specific requirements of wound healing. They have been shown to enhance wound healing, reduce bacterial colonization, and exhibit antibacterial properties, making them promising candidates for integration in wound dressings [5, 6].

In recent years, phytochemicals like carvacrol (CV; as an antimicrobial and wound-healing compound) have been reported as potential prospects for infection treatment [7]. CV is a phenolic monoterpenoid extracted from some plants such as oregano (*Origanum vulgare*), thyme (*Thymus vulgaris*), pepper (*Lepidium flavum*), and wild bergamot (*Citrus aurantium bergamia*). In addition to its potent antibacterial activity, research supports the role of CV in enhancing wound healing by 1) modulating the effect of inflammatory cytokines and oxidative stress, 2) enhancing re-epithelialization and angiogenesis, 3) improving the aggregation of collagen, and 4) modulating the growth of human fibroblast (HFF) cells and keratinocytes [8]. Research has shown that CV can destroy biofilms formed by *Salmonella Typhimurium* and inhibit biofilm formation of *Escherichia coli*. CV, in turn, demonstrates its dynamic antibiofilm action by causing changes in proteins involved in biofilm formation and antioxidant activity. It has also been reported to possess strong antimicrobial effects against various pathogens, including *E. coli*, methicillin-resistant *S. aureus*, and the yeast *Candida albicans* [5, 9-16]. These properties make CV a promising candidate as an alternative for fighting bacterial-associated infections.

As important lipid-based NPs, liposomes (LPs) are small vesicles exhibiting a high capacity for encapsulating both hydrophobic and hydrophilic antibiotics. LPs are naturally nontoxic and biologically degradable, and due to their amphiphilic and non-ionic structure, allow for the delivery of both hydrophobic and hydrophilic drugs. Research has shown the efficacy of LPs in enhancing the delivery of CV to the affected site. For example, Mir et al. studied the effect of hydrogels containing CV-encapsulating LPs as well as hydrogels containing free CV against methicillin-resistant *S. aureus* (MRSA). They evaluated the

delivery of CV via poly(ϵ -caprolactone) (PCL)-based liposomal NPs (i.e., PCL-LP-NPs) and found that CV release is remarkably increased when it is encapsulated in PCL-LP-NPs in the presence of bacterial lipase, while PCL-LP-NPs increase the anti-MRSA capacity of CV by two folds [17].

This study investigates the antibacterial effects of a CV-encapsulating liposomal nanosystem against three bacteria that can be involved in wound infections. The study 1) determines the rate of CV loading, entrapment, and release from the developed liposomal nanosystem, 2) evaluates CV's effects on *S. aureus*, *E. coli*, and *P. aeruginosa*, 3) compares the antibacterial effects of encapsulated and free CV, and 4) quantifies the cellular toxicity of the CV-encapsulating liposomal nanosystem. The purpose is to develop a nanocarrier with enhanced encapsulation rate and drug concentration, as well as a high liposome-to-drug ratio. The study further aims at reducing infections caused by *S. aureus*, *E. coli*, and *P. aeruginosa* by enhancing the developed nanoliposome's efficacy and minimizing CV's side effects against normal human foreskin fibroblast (HFF) cells. The motivation for this study is that fabricating such functional nanocarriers is a step forward in promoting the treatment of infectious wounds caused by bacterial strains.

MATERIALS AND METHODS

Materials

CV and P4417 -50Tab Phosphate Buffered Saline (PBS) tables were purchased from Sigma Aldrich (USA). Soy phosphatidylcholine (SPC), Tween-60, cholesterol (Chol), and methanol were purchased from Merck (Germany). Chloroform was purchased from Neutron Pharma-Chemical Co. (IRAN), and isopropyl was provided by Kimya Tejarat Roshan Co. (IRAN). HFF cells were provided by Yazd Reproductive Sciences Institute (Yazd, IRAN). All the statistical analyses were performed in Zeta Sizer (Malvern, USA), Essential FTIR (Python software foundation, USA), GraphPad Prism (Graph Pad Software Inc., USA), and Origin pro (Origin Lab Corporation, USA).

Methods

Preparation and fabrication of CV nanoliposomes

Various formulations of the liposomal nanosystem were synthesized using thin-film hydration (TFH) method (Table 1). Phospholipid

Table 1. Various formulations of SPC, Chol, and Tween® 60 to fabricate the CV-encapsulating liposomal nanosystem

No.	Formula	Molar ratio (%)	LPs/drug molar ratio	Drug's concentration
F1	SPC/Chol	70:30	15	0.5 mg/ml
F2	SPC/Chol	80:20	15	0.5 mg/ml
F3	SPC/Chol	60:40	15	0.5 mg/ml
F4	SPC/Chol	70:30	10	0.5 mg/ml
F5	SPC/Chol	80:20	10	0.5 mg/ml
F6	SPC/Chol	60:40	10	0.5 mg/ml
F7	SPC/Chol	70:30	15	1 mg/ml
F8	SPC/Chol/Tween60	42:18:40	20	4 mg/ml
F9	SPC/Chol/Tween60	50:25:25	20	4 mg/ml
F10	Tween60/Chol	70:30	20	5 mg/ml
F11	SPC/Chol/Tween60	60:25:15	15	2 mg/ml
F12	SPC/Chol/Tween60	60:25:15	10	1.5 mg/ml
F13	Tween60/Chol	70:30	10	4 mg/ml

(spc80), Chol, tween 60, and the desired amount of CV were dissolved in chloroform (as an organic solvent). To form a thin film layer, the organic solvent was evaporated in a rotary evaporator (ROTAVAP; Heidolph Instruments; Germany) under a vacuum condition. Regarding the hydrophobic nature of lipid compounds, LPs were formed due to the force applied after adding the aqueous phase during hydration (on the ROTAVAP for 45 min at 50 °C). Sonication was performed for 30 min using a probe sonicator (Ultrasonic Technology Development; UTD; IRAN), consisting of a 10-sec pause between “10-sec pulses” to achieve the optimum nano-sized small unilamellar vesicles (SUVs). The sonicated solution was passed through a 0.22 µm filter to remove impurities and separate the large-size samples from those with the intended and optimum size. Then, free (unloaded) CV present in the drug-containing liposomal suspension was removed by pouring the solution into the dialysis bag in a cold water bath with a temperature of 4 °C. Separation was carried out by stirring the solution for one hour in two 30-minute periods. After 30 min, the old buffer was replaced with a fresh buffer.

Analysis of the synthesized liposomal nanosystem CV entrapment into the liposomal nanocarrier

The encapsulation percentage of CV nanoliposomes was obtained by preparing the calibration chart of CV based on isopropyl by serial dilution method and using the following formula [18].

$$Entrapment\ Efficiency\ (\%EE) = \frac{Encapsulated\ Drug\ Concentration\ (\frac{mg}{ml})}{Primary\ used\ Drug\ Concentration\ (\frac{mg}{ml})} \times 100$$

CV release from the liposomal nanocarriers

CV release from nanoliposomes was measured under physiological conditions using a phosphate buffer at pH 7.4 and 37 °C. Briefly, 1 ml of the CV-containing liposomal solution was poured into the dialysis bag having 12 kDa pores and then placed in an isolated environment (i.e., a sterile falcon containing 10 cc of phosphate buffer) at 37 °C. Next, the buffer around the dialysis bag was sampled at different times (0.5, 1, 2, 3, 4, 5, 6, 7, 8, 24, 48, and 72 hr) and replaced with 1 ml of fresh buffer. The optical density (OD) absorbance at the maximum wavelength was then investigated by the spectrophotometer. Ultimately, the concentrations of the released CV at different times were measured and its graph was drawn using the calibration equation of the drug in PBS buffer [19].

Optimal formulation, and determination of size, dispersion index, and zeta potential (the DLS method)

After selecting the optimum formulation, dynamic light scattering (DLS) method was used to measure the hydrodynamic diameter, surface charge, and dispersion of LPs. DLS works by irradiating light rays to the sample, evaluating the intensity of received peaks, and measuring the velocity of movement of particles. The size of NPs is a key factor in drug accumulation in the target tissue, treatment efficiency, percolation from the vessel, and the transport and stability of nanocarriers. The zeta potential, dispersion index (PDI), and size of liposomal formulations were measured using the Zetasizer (model: Nano-Zeta Sizer

ES; Malvern Instruments; USA) at room temperature and an angle of 90°.

Field emission scanning electron microscopy (FE-SEM), Fourier transform infrared (FTIR) spectrum, and atomic force microscope (AFM)

The surface morphology of the nanocarriers (i.e., roughness, shape, smoothness, and aggregation) was investigated using FE-SEM. The molecular interactions of the compounds in the liposomal nanosystem and CV were investigated by the FTIR method. For this, the FTIR spectra of CV-free and CV-encapsulating LPs were obtained and compared with the final CV-encapsulating formulations. AFM was also used to prepare 3-D images of the liposomal nanosystems and investigate their surface topographies [20].

Antibacterial properties of the liposomal nanosystem

The antibacterial activity of the CV-encapsulating liposomal nanosystem and free CV against prenominate bacteria was investigated. The bacteria were standard strains purchased from Yazd University of Medical Sciences (YUMS; Yazd, IRAN) (Table 2).

Minimum inhibitory concentration (MIC) and minimal bactericidal concentration (MBC)

For measuring the MIC value, a 0.5 McFarland standard solution of bacteria was prepared using PBS and cultured bacteria, with an OD of 0.11. The tests were performed using 98-well plates, where 100 µl of the sterilized medium was first added to each plate. Then, 100 µl of sterilized samples were added through the serial dilution process. In the next stage, 5 µl of 0.5 McFarland standard solution was added to all the wells except the last well of all the rows. Furthermore, three wells having bacteria and medium were considered as a positive control, and three wells having only medium were regarded as a negative control. The experiment was repeated three times for each solution. The tests were performed on a separate plate for each bacterium. The plates were then kept at 37 °C for 24 hr. Eventually, the well with the MIC value

was obtained for each row through ELISA, and the overall result was obtained by averaging the results obtained from the three replications.

After determining the MIC value, the solutions from two wells (i.e., the wells located before the well that was previously considered as MIC) were swabbed on the sterile MHA medium and the plates were incubated for 18 hr in an incubator at 37 °C. Then, a dilution of the sample in which the bacterial growth was not visible was considered as MBC [21].

Cell culture and cellular cytotoxicity

The cells were cultured in appropriate containers with DMEM growth medium (Gibcob, Grand Island, NY, USA). The cultured cells were then allowed to grow and adhere under controlled conditions. Upon reaching confluency, cells were detached, counted, and transferred into a 96-well plate at desired densities. After incubation, the cells were treated with a medium containing different concentrations of the free and liposomal forms of CV. Free and liposomal CV concentrations were 953.7, 911.25, 760, 607.5, 303.75, 151.87, and 75.93 µg/ml.

After the drug exposure period, MTT solution was added to the cells, where metabolically active cells converted MTT into formazan. Following incubation, the formazan crystals were dissolved using a solvent, and the dissolved formazan absorbance was measured using an automated microplate reader (Biotech; USA), and the percentage of cell survival was calculated [20, 22-24].

Statistical analyses

All the MTT assay and MIC test results were analyzed using the one-way analysis of variance (ANOVA) test, and the graphs were drawn in GraphPad Prism software. The results were repeated at least three times, and the changes were calculated by averaging and reported by mean ± standard deviation (SD). The comparison tests used were two-way ANOVA, which was performed using the Padprism graph software, and $P < 0.05$ was considered as the minimum level of significance in each test.

Table 2. Bacteria used in the MIC test

Bacterium	Standard No.	Gram reaction
<i>Staphylococcus aureus</i>	25923	+
<i>Pseudomonas aeruginosa</i>	27853	-
<i>Escherichia coli</i>	25992	-

RESULTS

The effect of liposomal formulations on CV EE and release

To determine the optimal formulation of liposomal NPs, the range of CV loading on NPs, drug concentrations, and the ability of NPs to release CV were considered. The “EE” and “drug release” values were obtained for the alternative compositions of the components of NPs. For this, the “SPC-to-Chol” molar ratio, the “lipid-to-drug” ratio, and drug concentration and purity were evaluated as factors influencing the time-dependently loading of the drug on NPs. Likewise, Chol concentration was evaluated as a key factor influencing the release of CV from NPs (Table 4). According to Table 4, formulation F12 [SPC/Chol/Tween60-60:25:15; CV concentration: 1.5 mg/ml] achieved the best EE value of 81%.

CV standard calibration in isopropanol and PBS

Concerning the linear correlation between the absorption of CV and its various concentrations based on the Beer-Lambert law (indicating that both absorbance and concentration are directly proportional to each other), the graph demonstrating CV standard calibration in isopropanol and PBS was drawn using the Taylor Standard Series Method at the maximum wavelength of . The first-order differential equation for the drug was determined for use in calculating CV EE and release values. All the graphs had an acceptable “coefficient of determination” (R^2) above 99%. The drug loading in CV-containing liposomal NPs was reported as percentage (%) based on the standard graph.

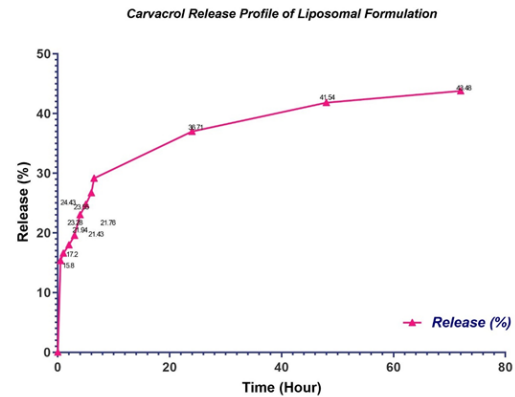


Fig. 1. The profile of CV release *in vitro* from the optimum liposomal formulations

The *in vitro* release of CV from optimal liposomal formulations

CV was released within 24 hr from liposomal NPs using the dialysis method at 37 °C. The release of CV from NPs was acceptable at 37 °C. As shown in Fig. 1, the release of CV follows a biphasic pattern. In the first phase, CV release is sharp from time “0” to “6 to 8” hr. Then, it enters a slow and linear phase over time, implying a semi-targeted release pattern. In this study, the release of CV from the liposomal nanosystem was reported from time “0” to “24 hr”. As demonstrated, CV release for all formulations is much higher in the initial stages. The rate of release is then reduced until it reached a stable release pattern. The formulation “F12” was considered the best formulation for drug release from liposomal NPs (Table 3).

Table 3. The optimum formulation of the CV-encapsulating liposomal nanosystem

Drug concentration	Formulation	Molar ratio	LPs/drug molar ratio
1.5 mg/ml	SPC:Chol: Tween60	60:25:15	10

Table 4. The CV EE of various formulations of Chol and SPC

No.	Formula	Molar ratio (%)	LPs/drug molar ratio	Drug concentration	EE %
F1	SPC: Chol	70:30	15	0.5 mg/ml	60.54
F2	SPC: Chol	80:20	15	0.5 mg/ml	58.85
F3	SPC: Chol	60:40	15	0.5 mg/ml	61.29
F4	SPC: Chol	70:30	10	0.5 mg/ml	59.34
F5	SPC: Chol	80:20	10	0.5 mg/ml	57.63
F6	SPC: Chol	60:40	10	0.5 mg/ml	60.11
F7	SPC: Chol	70:30	15	1mg/ml	77.24
F8	SPC: Chol: tween60	42:18:40	20	4mg/ml	No thin film formation
F9	SPC:Chol:tween60	50:25:25	20	4mg/ml	Unacceptable hydration
F10	Tween60:chol	70:30	20	5mg/ml	Unacceptable hydration
F11	SPC: Chol: Tween60	60:25:15	15	2mg/ml	Unacceptable hydration
F12	SPC: Chol: Tween60	60:25:15	10	1.5mg/ml	81±2
F13	Tween60: Chol	70:30	10	4mg/ml	75.55

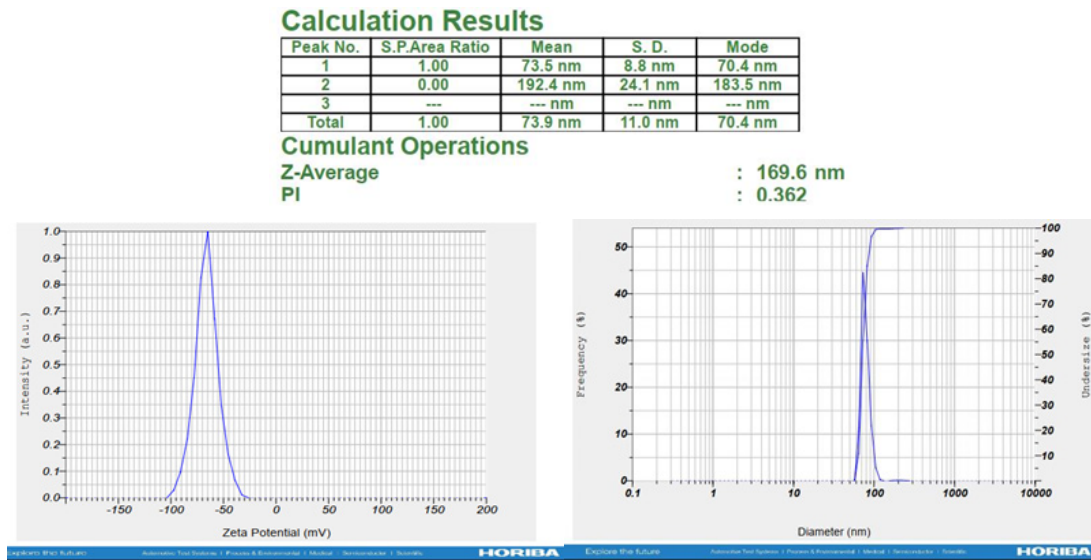


Fig. 2. The size and zeta potential of the optimum CV-encapsulating liposomal NPs

Characterization of CV-containing liposomal NPs

The size, zeta potential, and dispersion of NPs for the optimum formulation (F12) were measured by Zetasizer (HORIBA Scientific, Piscataway, New Jersey, NJ, USA). Based on the results, the mean size of liposomal NPs was 169 nm and their zeta potential was -24 mV (Fig. 2).

The morphology of LPs

Scanning electron microscope (SEM) images revealed the spherical shape of liposomal NPs which are appropriately distributed and their sizes are well agreeing with those obtained from

analyses with zetasizer.

FE-SEM (Fig. 3) and AFM (Fig. 4) images of liposomal nanosystems show the spherical morphology of LPs with clearly defined boundaries. There is also no aggregation of LPs. Notably, aggregation can adversely make LPs unstable and lead them to show unfavorable behaviors. In addition, the formed LPs are normal in terms of their morphological properties (i.e., a spherical shape, smoothness, and non-aggregation). AFM images clearly illustrate darker areas in the deeper parts and brighter areas on the surface of the NPs.

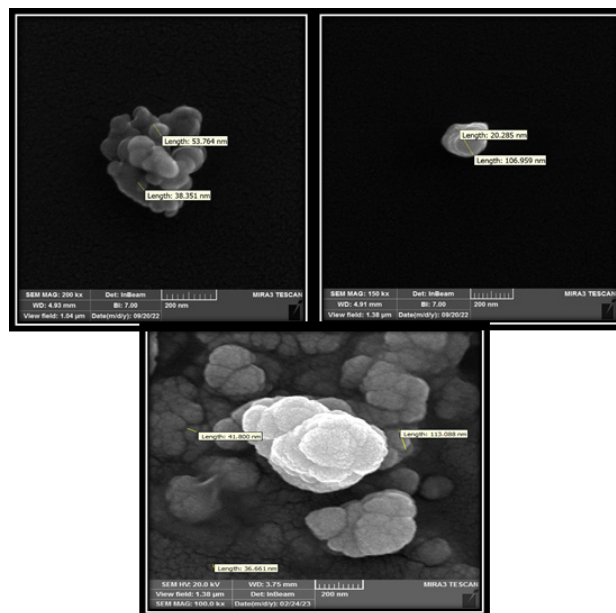


Fig. 3. FESEM images of optimal CV-encapsulating liposomal nanosystems

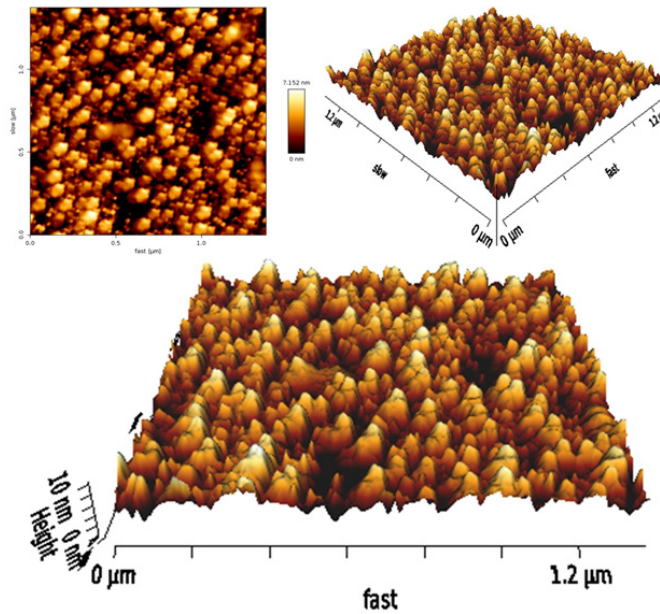


Fig. 4. SEM images illustrating the morphology of CV-encapsulating liposomal NPs

FTIR results

The FTIR spectrum for free and nano encapsulated CV

The FTIR spectrum for CV revealed characteristic peaks in the region “3382.73 ” (due to the stretching vibration of the phenolic group (O-H)), “2960.85 ” (due to C-H stretching in the branched alkanes), “1589.83 ” (due to the C-C stretching band), “1459-1421 ” (due to the bending vibration of OH), “1302.40 ” (due to the isopropyl group), a strong band at “1252.31 ” due to C-O-C stretching, and ultimately in the region “812.35 ” (due to aromatic C-H bending) (Fig. 5) (Table 5).

Table 5. The major FTIR absorptions

Band	Assignment
3382.73	O-H
2960.85	C-H stretching band
1589.83	C-C stretching band
1459-1421	OH bending
1302.40	(CCH ₃) ₂
1252.31	C-O-C stretching
812.35	C-H bending

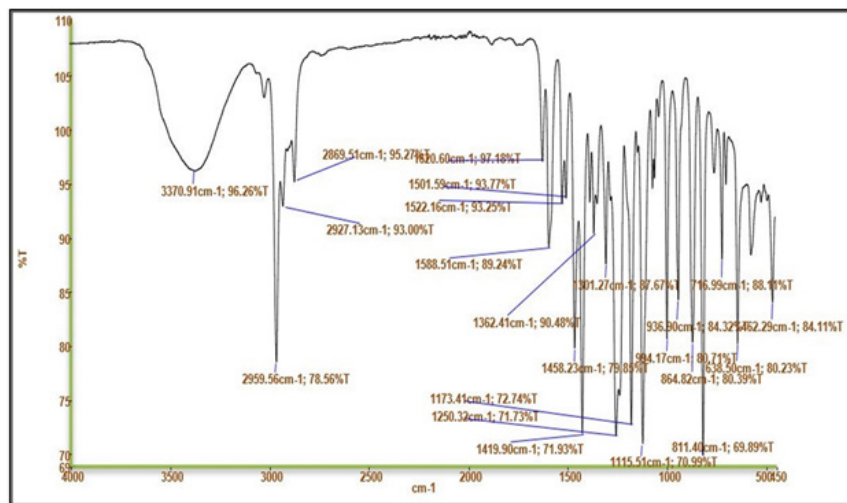


Fig. 5. FTIR spectrum of CV

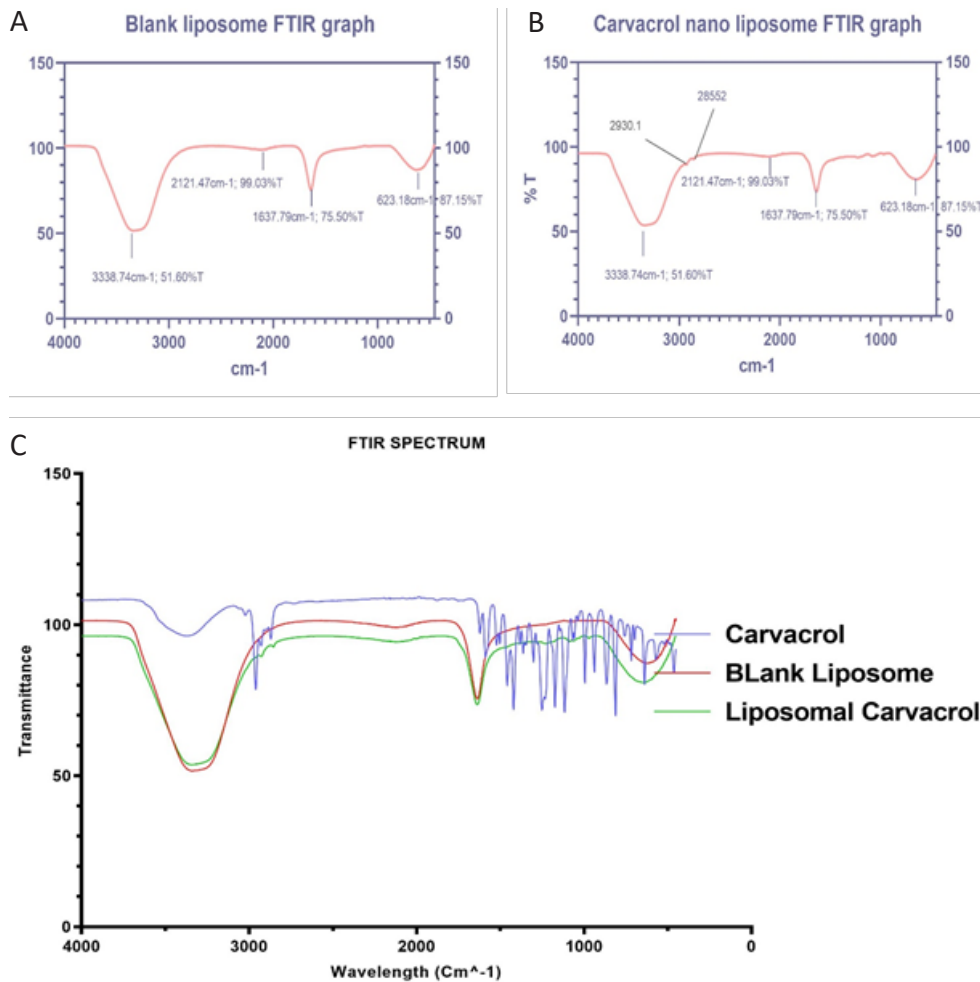


Fig. 6. FTIR spectrum for “blank LPs” (A), “CV-encapsulating LPs” (B), and merged state (C)

FTIR spectrum for the liposomal blank system, CV-encapsulating LPs, and merged FTIR spectra

FTIR spectra for “blank LPs” and “CV-encapsulating LPs” are shown in Fig. 6-A and 6-B, respectively. As shown in Fig. 6-B, there are two index peaks (2930 and 2855) for CV-encapsulating LPs. The FTIR spectra for both “blank LPs” and “CV-encapsulating LPs” show a trivial shift of the peaks towards the lower wave number side, presumably due to weak hydrogen C illustrates the merged FTIR spectra for “CV”, “blank LPs”, and “CV-encapsulating LPs”.

Microbial assessments

The efficacy of CV-encapsulating LPs in inhibiting the growth of *S. aureus* compared to free CV is shown in Fig. 7-A.

As illustrated, the inhibitory effect of both “free CV” and “CV-encapsulating LPs” is concentration-

dependently increased. At concentrations of 953.7, 911.25, 760, and 607.50 $\mu\text{g}/\text{mL}$, the inhibitory effect of both “free CV” and “CV-encapsulating LPs” is nearly equal. However, at concentrations below 303.76 $\mu\text{g}/\text{mL}$, “CV-encapsulating LPs” outperform “free CV” in inhibiting the growth of *S. aureus*, resulting in a significant difference between the two groups. Likewise, as shown in Fig. 7-B, the MIC value for “CV-encapsulating LPs” (151.87) is much less than that for “free CV” (607.5), implying that encapsulated CV exhibits a much stronger antibacterial effect on *S. aureus* compared to its free form.

The efficacy of CV-encapsulating LPs in inhibiting the growth of *E. coli* compared to free CV is shown in Fig. 8-A.

As depicted, the inhibitory effect of both “free CV” and “CV-encapsulating LPs” is concentration-dependently increased. At concentrations of

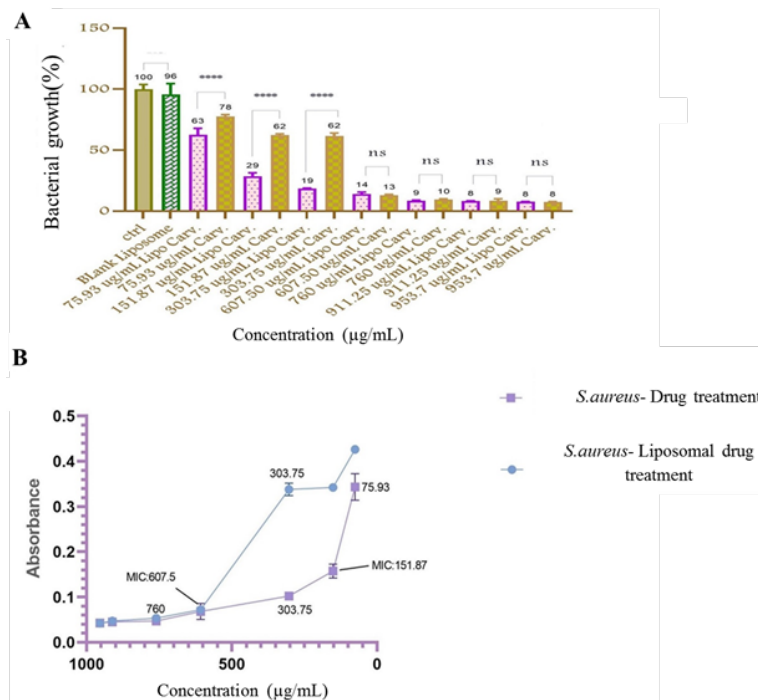


Fig. 7. A) The efficacy of “free CV” and “CV-encapsulating LPs” in inhibiting the growth of *S. aureus* based on the MIC test. B) MIC value for *S. aureus*

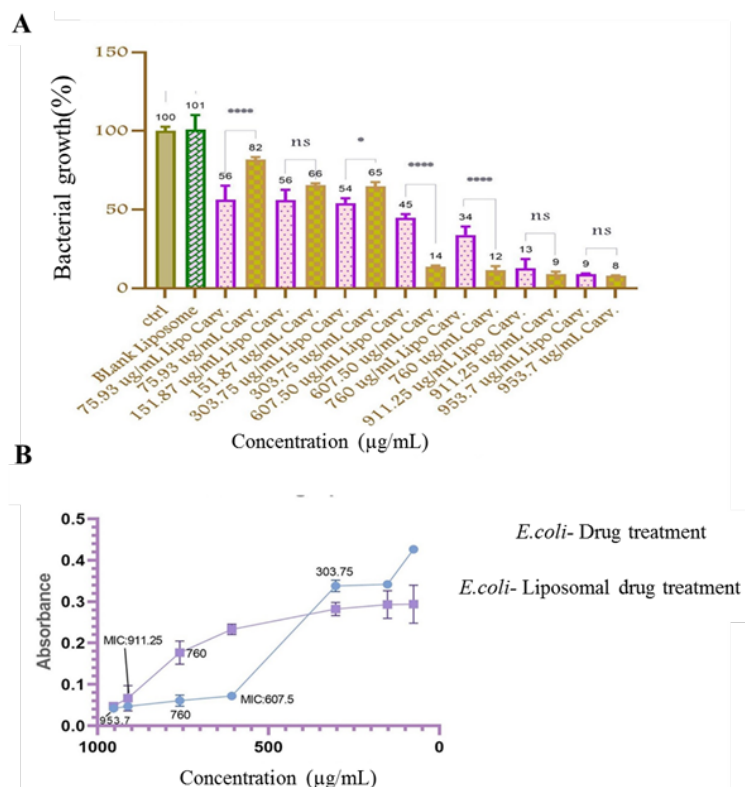


Fig. 8. A) The efficacy of “free CV” and “CV-encapsulating LPs” in inhibiting the growth of *E. coli* based on the MIC test. B) MIC value for *E. coli*

953.7 and 911.25 µg/mL, the inhibitory effect of both “free CV” and “CV-encapsulating LPs” is nearly equal. However, at concentrations of 760 and 607.50 µg/mL, the efficacy of “free CV” in inhibiting the growth of *E. coli* is higher than that of “CV-encapsulating LPs”. Furthermore, as shown in Fig. 8-B, the MIC value for “free CV” (607.5) is much less than that for “CV-encapsulating LPs” (911.25), suggesting that “free CV” outperforms “encapsulated CV” in inhibiting the growth of *E. coli*.

The efficacy of CV-encapsulating LPs in inhibiting the growth of *P. aeruginosa* compared to free CV is shown in Fig. 9.

As demonstrated in Fig. 9-A, the inhibitory effect of “free CV” is much higher than that of “CV-encapsulating LPs”. Except for their highest concentration (953.7 µg/mL), “CV-encapsulating LPs” at other concentrations not only exhibit no growth-inhibitory effects but also result in the higher growth of *P. aeruginosa*. Furthermore, as shown in Fig. 9-B, “CV-encapsulating LPs”

exhibit growth-inhibitory effects at their highest concentration (953.7 µg/mL). Thus, the MIC value for “free CV” is 607.5 and that of “CV-encapsulating LPs” is 953.7.

Cytotoxicity assay of CV-encapsulating LPs

Fig. 10 shows the effects of “free CV” and “CV-encapsulating LPs” on the survival of HFF cells after 24 hr, according to the MTT assay results.

The obtained data suggest that blank LPs (compared to the control group) exhibit no cytotoxicity against HFF cells, with insignificant differences between the two groups. However, “CV-encapsulating LPs”, compared to “free LPs” at the same concentrations, not only possess no cytotoxicity against HFF cells but also results in the higher growth and survival of these cells. There is a significant difference between this finding and the data obtained from treatments with CV which are associated with triggered apoptosis.

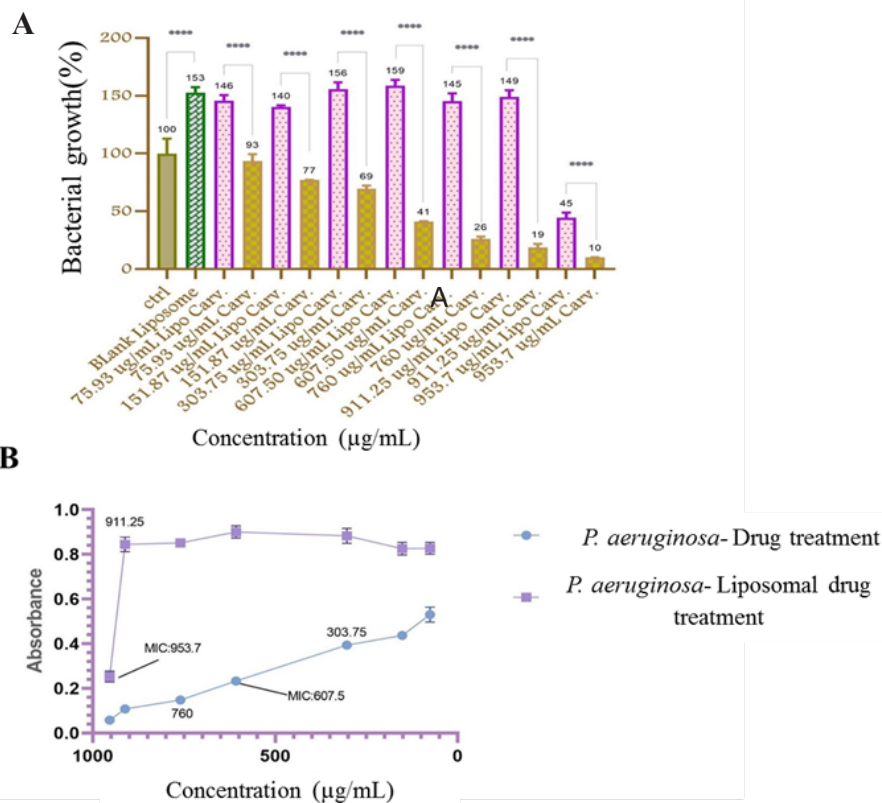


Fig. 9. A) The efficacy of “free CV” and “CV-encapsulating LPs” in inhibiting the growth of *P. aeruginosa* based on the MIC test. B) MIC value for *P. aeruginosa*

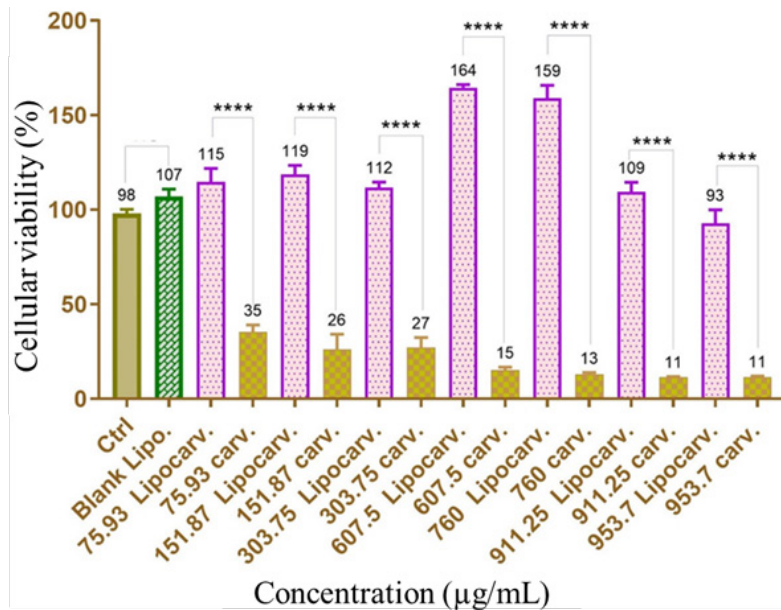


Fig. 10. The effects of “free CV” and “CV-encapsulating LPs” on the survival of human foreskin fibroblast (HFF) cells after 24 hr, according to the MTT assay results

DISCUSSION

Wound infections are a significant concern due to their association with morbidity and mortality, especially in developing countries. *S. aureus*, *P. aeruginosa*, and *E. coli* are commonly isolated pathogens in wound infections. *S. aureus* and *P. aeruginosa* are the predominant species in wound infections and have been reported to disrupt the wound-healing process [25-28].

Recent advancements in the treatment of wound infections have focused on developing more efficient therapeutics for chronic and acute wound infections. The distinctive biological, non-sterile wound environment and the complex wound-healing system have provoked the exploration of unconventional and non-antibiotic treatments, particularly the antimicrobial potential of natural agents such as essential oils. Additionally, innovative wound dressings have been reported to provide a favorable environment and deliver active ingredients to the wounded site, thereby accelerating the healing process [29].

In this study, CV was encapsulated by LPs to increase its stability due to its volatility, improve its release in the affected site, reduce its toxicity toward normal HFF cells, and multiply its antibacterial effect on the bacteria. The purpose was to develop a potent nanocarrier exhibiting excellent drug EE, controlled drug release, and trivial cytotoxicity of the encapsulated drug

against healthy tissues and cells. For this purpose, a liposomal nanosystem was fabricated using CV, SPC, Chol, and Tween-60. In the fabricated nanosystem, SPC enhances the drug permeability by improving the fluidity and results in a better response to the administered drug. Due to its structural similarity with biological membrane phospholipids, SPC is frequently employed in various drug delivery formulations. SPC seems to be a suitable molecule for designing liposomal formulations against various diseases such as cancer. For example, Di sotto et al. reported that SPC enhances the bioavailability and absorption of β -caryophyllene (*CRY* – a natural sesquiterpene) by cancer cells. They found that, at lower SPC/*CRY* (mol/mol) ratios, the fabricated SPC-*CRY*-LPs can remarkably potentiate the antiproliferative capacity of *CRY* in “MDA-MB-468” and “HepG2” cells [30]. The ability of SPC to enhance drug permeability has been reported elsewhere for wound infection. For example, El-Gizway et al. reported the ability of transpersonal gels incorporating deferoxamine (*DFO* – an effective *HIF-1 α* stabilizer) and SPC in enhancing the permeability of *DFO* for cutaneous wound healing in rats’ diabetic pressure ulcers, implying the capacity of these formulations for the treatment of human diabetic ulcers [31]. However, an increase in the concentration of Chol in the final formulation reduces drug release due to a decline in the fluidity of the membrane of LPs [32].

Thus, various ratios of Chol/SPC/Tween-60 were investigated to achieve the optimal formulation (i.e., "F12", [Chol/SPC/Tween-60; ratio: 25:60:15; CV EE: 81%; CV release: 43.48%]) for further experiments. Notably, adding surfactants such as Tween-60 increases the flexibility of vesicles and the stability of LPs. Due to its hydrophilic head group, Tween 60 declines the high interfacial tension of the LPs, culminating in a more invariant polydispersity index (PDI) and volume median diameter (VMD) [33].

The volume of drug release from the delivery system is a key aspect in fabricating an optimal system exhibiting a desired drug release pattern. Owing to its small molecular size, CV is readily released from the dialysis tubing with 12 kDa pores. The initial prompt release of CV is controlled by the diffusion mechanism, i.e., the concentration gradient of CV between LPs and the buffer around the dialysis bag, while its gradual release in the second phase is due to the controlled release from the bilayer membrane of the LPs [34, 35]. In this study, the size of all formulations (i.e., blank LPs and CV-loaded LPs) was from 76 to 169 nm. Research shows that the best size of NPs for use in pharmaceutical systems is from 50 to 200 nm [36], and nanosystems with a diameter of 50 to 80 nm exhibit a better capacity to escape from mononuclear phagocytes [37]. The negative charge of all formulations implies the formation of anionic LPs that possess attributes such as enhanced stability in solution and improved endocytosis [38].

In this study, both "CV-encapsulating LPs" and "free CV" exhibited a nearly equal antibacterial effect on *S. aureus* at higher concentrations. However, the effect of "CV-encapsulating LPs" on *S. aureus* was significantly higher than that of free CV in the lower concentrations. Similarly, both "CV-encapsulating LPs" and "free CV" exhibited an equal concentration-dependently killing effect on *E. coli* at higher concentrations. However, the free form of CV outperformed "CV-encapsulating LPs" in killing *E. coli* at lower concentrations. In a similar study, Liolios et al. investigated the antimicrobial effect of CV-encapsulating LPs against four Gram-negative and Gram-positive bacteria. They found that the antibacterial properties of CV are improved when it is entrapped in the LPs [39]. By contrast, a 2020 study by Cacciatore et al. revealed that the free form of CV has a better effect on food pathogens

attached to steel than the encapsulated form of CV [40]. However, CV-encapsulating polymeric nanocapsules exhibit bactericidal effects on *S. aureus*, *E. coli*, and *Salmonella bacteria*.

For *P. aeruginosa*, the antibacterial effect of free CV was much higher than that of CV-encapsulating LPs. Except for its highest concentration (i.e., 953.7 µg/ml), CV-encapsulating LPs exhibited no inhibitory effects in other concentrations where the growth of *P. aeruginosa* was expanded. This finding is in contrast with the results reported by Gobin et al. who investigated the effect of gallic acid, CV, and curcumin on the formation of biofilm by two common bacteria involved in infectious wounds (i.e., *P. aeruginosa* and *S. aureus*). They found that CV can eliminate the biofilm produced by both bacterial strains [41]. Such a discrepancy between the results may be due to the difference in the concentration of CV between the studies, where the concentration of CV in the study by Gobin et al. is nearly two times that in the present study. The antibacterial effect of CV and thymol against *P. aeruginosa* and *S. aureus* has been investigated elsewhere by Lambert et al. [42].

The MTT assay results revealed that the encapsulated form of CV enhances the growth of HFF cells, thereby improving wound healing. In the present study, MTT assay results further showed that blank LPs and CV-encapsulating LPs possess no cytotoxicity against HFF cells, and encapsulating CV in LPs removes the toxicity of CV at the studied concentrations. However, at similar concentrations, free CV was found to exert some degree of cytotoxicity against HFF cells, particularly at higher concentrations. This finding agrees with the results reported by Yao et al. in 2021, where they found that free CV leads to the death of HFF cells at higher concentrations [43].

CONCLUSION AND PROSPECTS

In this study, the optimum CV-encapsulation liposomal nanosystems were fabricated and characterized for use in the treatment of wound infections. The study revealed that various concentrations of CV-LPs inhibit the growth of *S. aureus* and *E. coli* involved in most severe wound infections. Furthermore, encapsulating CV in LPs reduced its cytotoxicity against HFF cells even at higher concentrations. Collectively, these results imply the use of CV-LPs as a promising nanosystem in alleviating and healing infections. However, future studies are recommended to 1) investigate

CV-LPs on a mouse model of wound infection, 2) use CV-LPs in the form of hydrogel dressings, 3) evaluate the effect of CV-encapsulating liposomal nanosystems on bacteria involved in wound infection, and 4) investigate the synergistic effect of CV-LPs and antibiotics for the treatment of antibiotic-resistant bacteria.

ACKNOWLEDGMENTS

The present research was approved by the ethics committee of the Biotechnology Research Center, International Campus, Shahid Sadoughi University of Medical Sciences, Yazd, Iran. We kindly appreciate Sanaz Raeisi, Mahdieh Parsaeian, Niloofar Dehghani, Mahdieh Tajardoost, and Shahin Shahi, as well as the Research and Clinical Center for Infertility (Yazd, Iran) and Shahid Sadoughi University of Medical Sciences (SSUMS) for scientific contribution during the project.

CONFLICTS OF INTEREST

The authors declare no conflicts of interest.

REFERENCES

- Beygi M, Oroojalian F, Hosseini SS, Mokhtarzadeh A, Kesharwani P, Sahebkar A. Recent progress in functionalized and targeted polymersomes and chimeric polymeric nanotheranostic platforms for cancer therapy. *Prog Mater Sci.* 2023;101209.
- Oroojalian F, Beygi M, Baradaran B, Mokhtarzadeh A, Shahbazi MA. Immune cell membrane-coated biomimetic nanoparticles for targeted cancer therapy. *Small.* 2021;17(12):2006484.
- Zolghadri S, Beygi M, Mohammad TF, Alijanianzadeh M, Pillaiyar T, Garcia-Molina P, et al. Targeting tyrosinase in hyperpigmentation: current status, Limitations and future promises. *Biochem Pharmacol.* 2023;115574.
- Oroojalian F, Karimzadeh S, Javanbakht S, Hejazi M, Baradaran B, Webster TJ, et al. Current trends in stimuli-responsive nanotheranostics based on metal-organic frameworks for cancer therapy. *Mater Today.* 2022;57:192-224.
- Karimi MA, Dadmehr M, Hosseini M, Korouzhdehi B, Oroojalian F. Sensitive detection of methylated DNA and methyltransferase activity based on the lighting up of FAM-labeled DNA quenched fluorescence by gold nanoparticles. *RSC Adv.* 2019;9(21):12063-12069.
- Hosseini Motlagh NS, Sharifi E, Hghiralsadat BF, Sardari Zarchi M, Yaghoubi F, Oroojalian F. Investigation and comparison of laser and ultrasound effects on the temperature increasing of the solutions containing graphene oxide nanoparticles for thermal treatment of osteosarcoma cancer cells. *Nanomed J.* 2023;10(4):313-322.
- Mir M, Permana AD, Ahmed N, Khan GM, ur Rehman A, Donnelly RF. Enhancement in site-specific delivery of carvacrol for potential treatment of infected wounds using infection responsive nanoparticles loaded into dissolving microneedles: A proof of concept study. *Eur J Pharm Biopharm.* 2020;147:57-68.
- Costa MF, Durço AO, Rabelo TK, Barreto RdSS, Guimarães AG. Effects of Carvacrol, Thymol and essential oils containing such monoterpenes on wound healing: A systematic review. *J Pharm Pharmacol.* 2019;71(2):141-155.
- Trevisan DAC, Campanerut-Sa PAZ, da Silva AF, Batista AFP, Seixas FAV, Peralta RM, et al. Action of carvacrol in Salmonella Typhimurium biofilm: A proteomic study. *J Appl Biomed.* 2020;18(4):106-114.
- Trevisan DAC, Silva Afd, Negri M, Abreu Filho BAd, Machinski Junior M, Patussi EV, et al. Antibacterial and antibiofilm activity of carvacrol against Salmonella enterica serotype Typhimurium. *Braz J Pharm Sci.* 2018;54.
- Omidi M, Malakoutian M, Choolaei M, Oroojalian F, Haghirsadat F, Yazdian F. A Label-Free detection of biomolecules using micromechanical biosensors. *Chin Phys Lett.* 2013;30(6):068701.
- Azizi M, Tavana M, Farsi M, Oroojalian F. Yield performance of Lingzhi or Reishi medicinal mushroom, *Ganoderma lucidum* (W. Curt.: Fr.) P. Karst.(higher Basidiomycetes), using different waste materials as substrates. *Int J Med Mushrooms.* 2012;14(5).
- Azizi M, Chizzola R, Ghani A, Oroojalian F. Composition at different development stages of the essential oil of four Achillea species grown in Iran. *Nat Prod Commun.* 2010;5(2):1934578X1000500224.
- Chizzola R, Saeidnejad AH, Azizi M, Oroojalian F, Mardani H. Bunium persicum: variability in essential oil and antioxidants activity of fruits from different Iranian wild populations. *Genet Resour Crop Evol.* 2014;61:1621-1631.
- Ebrahimpour M, Akhlaghi M, Hemati M, Ghazanfary S, Shahriary S, Ghalekohneh SJ, et al. In vitro evaluation and comparison of anticancer, antimicrobial, and antifungal properties of thyme niosomes containing essential oil. *Nanomed J.* 2022;9(4).
- Rashidi A, Omidi M, Choolaei M, Nazarzadeh M, Yadegari A, Haghiersadat F, et al. Electromechanical properties of vertically aligned carbon nanotube. *Adv Mat Res.* 2013;705:332-336.
- Mir M, Ahmed N, Permana AD, Rodgers AM, Donnelly RF, Rehman AU. Enhancement in site-specific delivery of carvacrol against methicillin resistant Staphylococcus aureus induced skin infections using enzyme responsive nanoparticles: a proof of concept study. *Pharmaceutics.* 2019;11(11):606.
- Nia AH, Behnam B, Taghavi S, Oroojalian F, Eshghi H, Shier WT, et al. Evaluation of chemical modification effects on DNA plasmid transfection efficiency of single-walled carbon nanotube-succinate-polyethylenimine conjugates as non-viral gene carriers. *Med Chem Comm.* 2017;8(2):364-375.
- Pishavar E, Oroojalian F, Ramezani M, Hashemi M. Cholesterol-conjugated PEGylated PAMAM as an efficient nanocarrier for plasmid encoding interleukin-12 immunogene delivery toward colon cancer cells. *Biotechnol Prog.* 2020;36(3):e2952.
- Oroojalian F, Rezayan AH, Mehrnejad F, Nia AH, Shier WT, Abnous K, et al. Efficient megalin targeted delivery to renal proximal tubular cells mediated by modified-polymyxin B-polyethylenimine based nano-gene-carriers. *Mater Sci Eng C.* 2017;79:770-782.
- Rahimizadeh M, Eshghi H, Shiri A, Ghadamyari Z, Matin MM, Oroojalian F, et al. Fe (HSO 4) 3 as an efficient catalyst for diazotization and diazo coupling reactions. *J Korean Chem Soc.* 2012;56(6):716-9.
- Oroojalian F, Rezayan AH, Shier WT, Abnous K, Ramezani M. Megalin-targeted enhanced transfection efficiency in cultured human HK-2 renal tubular proximal cells using aminoglycoside-carboxyalkyl-polyethylenimine-containing nanoplexes. *Int J Pharm.* 2017;523(1):102-20.
- Gholami Z, Dadmehr M, Jelodar NB, Hosseini M, Parizi AP. One-pot biosynthesis of CdS quantum dots through in vitro regeneration of hairy roots of *Rhaphanus sativus* L. and their apoptosis effect on MCF-7 and AGS cancerous human cell lines. *Mater Res Express.* 2020;7(1):015056.
- Pourpirali R, Mahmoudnezhad A, Oroojalian F, Zarghami N, Pilehvar Y. Prolonged proliferation and delayed senescence of the adipose-derived stem cells grown on the electrospun composite nanofiber co-encapsulated with

- TiO₂ nanoparticles and metformin-loaded mesoporous silica nanoparticles. *Int J Pharm.* 2021;604:120733.
25. Alves PM, Al-Badi E, Withycombe C, Jones PM, Purdy KJ, Maddocks SE. Interaction between *Staphylococcus aureus* and *Pseudomonas aeruginosa* is beneficial for colonisation and pathogenicity in a mixed biofilm. *Pathog Dis.* 2018;76(1).
 26. Giacometti A, Cirioni O, Schimizzi A, Del Prete M, Barchiesi F, D'Errico M, et al. Epidemiology and microbiology of surgical wound infections. *J Clin Microbiol.* 2000;38(2):918-922.
 27. Puca V, Marulli RZ, Grande R, Vitale I, Niro A, Molinaro G, et al. Microbial species isolated from infected wounds and antimicrobial resistance analysis: Data emerging from a three-years retrospective study. *Antibiotics.* 2021;10(10):1162.
 28. Moghaddam FA, Ebrahimian M, Oroojalian F, Yazdian-Robati R, Kalalinia F, Tayebi L, et al. Effect of thymoquinone-loaded lipid-polymer nanoparticles as an oral delivery system on anticancer efficiency of doxorubicin. *J Nanostructure Chem.* 2021:1-12.
 29. Negut I, Grumezescu V, Grumezescu AM. Treatment Strategies for Infected Wounds. *Molecules.* 2018;23(9).
 30. Di Sotto A, Paolicelli P, Nardoni M, Abete L, Garzoli S, Di Giacomo S, et al. SPC liposomes as possible delivery systems for improving bioavailability of the natural sesquiterpene β -caryophyllene: lamellarity and drug-loading as key features for a rational drug delivery design. *Pharmaceutics.* 2018;10(4):274.
 31. El-Gizawy SA, Nouh A, Saber S, Kira AY. Deferoxamine-loaded transfersomes accelerates healing of pressure ulcers in streptozotocin-induced diabetic rats. *J Drug Deliv Sci Technol.* 2020;58:101732.
 32. Ruwizhi N, Aderibigbe BA. The efficacy of cholesterol-based carriers in drug delivery. *Molecules.* 2020;25(18):4330.
 33. Khan I, Needham R, Yousaf S, Houacine C, Islam Y, Bnyan R, et al. Impact of phospholipids, surfactants and cholesterol selection on the performance of transfersomes vesicles using medical nebulizers for pulmonary drug delivery. *J Drug Deliv Sci Technol.* 2021;66:102822.
 34. Kamboj S, Saini V, Bala S. Formulation and characterization of drug loaded nonionic surfactant vesicles (niosomes) for oral bioavailability enhancement. *Sci World J.* 2014;2014.
 35. Panwar P, Pandey B, Lakhera P, Singh K. Preparation, characterization, and in vitro release study of albendazole-encapsulated nanosize liposomes. *Int J Nanomedicine.* 2010:101-108.
 36. Maja L, Željko K, Mateja P. Sustainable technologies for liposome preparation. *J Supercrit Fluids.* 2020;165:104984.
 37. Danaei M, Dehghankhold M, Ataei S, Hasanzadeh Davarani F, Javanmard R, Dokhani A, et al. Impact of particle size and polydispersity index on the clinical applications of lipidic nanocarrier systems. *Pharmaceutics.* 2018;10(2):57.
 38. Neves LF, Duan J, Voelker A, Khanal A, McNally L, Steinbach-Rankins J, et al. Preparation and optimisation of anionic liposomes for delivery of small peptides and cDNA to human corneal epithelial cells. *J Microencapsul.* 2016;33(4):391-399.
 39. Liolios C, Gortzi O, Lalas S, Tsaknis J, Chinou I. Liposomal incorporation of carvacrol and thymol isolated from the essential oil of *Origanum dictamnus* L. and in vitro antimicrobial activity. *Food Chem.* 2009;112(1):77-83.
 40. Cacciatore FA, Dalmás M, Maders C, Isaia HA, Brandelli A, da Silva Malheiros P. Carvacrol encapsulation into nanostructures: Characterization and antimicrobial activity against foodborne pathogens adhered to stainless steel. *Food Res Int.* 2020;133:109143.
 41. Gobin M, Proust R, Lack S, Duciel L, Des Courtils C, Pauthe E, et al. A combination of the natural molecules gallic acid and carvacrol eradicates *P. aeruginosa* and *S. aureus* mature biofilms. *Int J Mol Sci.* 2022;23(13):7118.
 42. Lambert R, Skandamis PN, Coote PJ, Nychas GJ. A study of the minimum inhibitory concentration and mode of action of oregano essential oil, thymol and carvacrol. *J Appl Microbiol.* 2001;91(3):453-462.
 43. Yao N, Xu Q, He J-K, Pan M, Hou Z-F, Liu D-D, et al. Evaluation of *Origanum vulgare* essential oil and its active ingredients as potential drugs for the treatment of toxoplasmosis. *Front Cell Infect Microbiol.* 2021;11:793089.